

ARTICLE



Nodal cytotoxic peripheral T-cell lymphoma occurs frequently in the clinical setting of immunodysregulation and is associated with recurrent epigenetic alterations

Alina Nicolae^{1,2,3}, Justine Bouilly⁴, Diane Lara^{3,5}, Virginie Fataccioli^{3,6}, François Lemonnier^{3,7}, Fanny Drieux^{8,9}, Marie Parrens¹⁰, Cyrielle Robe^{3,6}, Elsa Poullot^{3,6}, Bettina Bisig⁴, Céline Bossard¹¹, Audrey Letourneau⁴, Edoardo Missiaglia^{4,12}, Christophe Bonnet¹³, Vanessa Szablewski¹⁴, Alexandra Traverse-Glehen¹⁵, Marie-Hélène Delfau-Larue^{3,16}, Laurence de Leval^{4,17} and Philippe Gaulard^{3,6,17}✉

© The Author(s), under exclusive licence to United States & Canadian Academy of Pathology 2022

Nodal peripheral T-cell lymphoma, not otherwise specified (PTCL, NOS) with cytotoxic phenotype is overall rare, with most reports coming from Asia. Given its elusive pathobiology, we undertook a clinicopathological and molecular study of 54 Western patients diagnosed with PTCL, NOS expressing cytotoxic molecules, within a lymph node. More commonly males (M/F-2,6/1) with median age of 60 years were affected. Besides lymphadenopathy, 87% of patients had ≥ 1 involved extranodal site. High-stage disease (III-IV), International Prognostic Index >2 , B symptoms, LDH level, and cytopenia(s) were observed in 92, 63, 67, 78, and 66% of cases, respectively. Ten patients had a history of B-cell malignancies, one each of myeloid neoplasm, breast or prostate cancer, and 4 others had underlying immune disorders. Most patients (70%) died, mostly of disease, with a median overall survival of 12.7 months. Immunophenotypically, the neoplastic lymphocytes were T-cell receptor (TCR) $\alpha\beta$ + (47%), TCR-silent (44%) or TCR $\gamma\delta$ + (10%), commonly CD8 + (45%) or CD4-CD8- (32%). All except one had an activated cytotoxic profile, and 95% were subclassified into PTCL-TBX21 subtype based on CXCR3, TBX21, and GATA3 expression pattern. Seven patients (13%) disclosed EBER + tumor cells. Targeted DNA deep-sequencing (33 cases) and multiplex ligation-dependent reverse transcription-polymerase chain reaction assay (43 cases) identified frequent mutations in epigenetic modifiers (73%), including *TET2* (61%) and *DNMT3A* (39%), recurrent alterations affecting the TCR (36%) and JAK/STAT (24%) signaling pathways and *TP53* mutations (18%). Fusion transcripts involving *VAV1* were identified in 6/43 patients (14%). Patients with nodal cytotoxic PTCL, NOS have an aggressive behavior and frequently present in a background of impaired immunity, although the association with Epstein-Barr virus is rare. The recurrent alterations in genes involved in DNA methylation together with genes related to cytokine or TCR signaling, suggest that co-operation of epigenetic modulation with cell-signaling pathways plays a critical role in the pathogeny of these lymphomas.

Modern Pathology (2022) 35:1126–1136; <https://doi.org/10.1038/s41379-022-01022-w>

INTRODUCTION

Mature T- and NK-cell lymphomas are uncommon and highly heterogeneous, with 29 distinct entities described in the 2017 WHO classification, encompassing 7–10% of non-Hodgkin lymphomas^{1,2}. They involve nodal and extranodal sites and often follow an aggressive clinical course^{1,3}. Improved knowledge of T-cell ontogeny combined with integrated genomic and transcriptomic approaches have illuminated T-cell lymphomas' biology and oriented towards the putative cell of origin for some entities.

Cytotoxic $\alpha\beta$ or $\gamma\delta$ T and NK cells represent subsets of lymphocytes with major roles in host epithelial immune surveillance, in the elimination of virus-infected and neoplastic transformed cells⁴. The "killing" of target cells occurs by release of granule-associated cytotoxic proteins into the immunological synapse. The key molecular players in this process are perforin, a pore-forming protein; granzymes, a family of granule-bound serine proteases; and T-cell intracellular antigen-1 (TIA-1) which regulates several components of cell death pathways^{4,5}. Regardless of their activation status, cytotoxic T and NK cells

¹Department of Pathology, Hautepierre, University Hospital Strasbourg, Strasbourg, France. ²INSERM, IRFAC / UMR-S1113, ITI InnoVec, FHU ARRIMAGE, FMST, University of Strasbourg, Strasbourg, France. ³INSERM U955, Université Paris-Est, Créteil, France. ⁴Institute of Pathology, Department of Laboratory Medicine and Pathology, Lausanne University Hospital (CHUV) and Lausanne University, Lausanne, Switzerland. ⁵Service d'Hématologie, Centre Hospitalier Robert Boulin, Libourne, France. ⁶Département de Pathologie, Groupe Hospitalier Henri Mondor, AP-HP, Créteil, France. ⁷Unité Hémopathies lymphoïdes, Groupe Hospitalier Henri Mondor, AP-HP, Créteil, France. ⁸INSERM U1245, Centre Henri Becquerel, Rouen, France. ⁹Service d'Anatomie et Cytologie Pathologiques, Centre Henri Becquerel, Rouen, France. ¹⁰Département de Pathologie, Hôpital Haut-Lévêque, Université de Bordeaux, INSERM, BaRITon, U1053, F-33000 Bordeaux, France. ¹¹Service d'Anatomie et Cytologie Pathologiques, CHU de Nantes, Nantes, France. ¹²Swiss Institute of Bioinformatics, Lausanne, Switzerland. ¹³Hématologie clinique, CHU Sart-Tilman Liège, Liège, Belgique. ¹⁴Service d'Anatomopathologie, CHU Montpellier, Montpellier, France. ¹⁵Pathology Department, Centre Hospitalier Lyon-Sud, Pierre-Bénite, France. ¹⁶Département d'Hématologie et Immunologie Biologique, Groupe Hospitalier Henri Mondor, AP-HP, Créteil, France. ¹⁷These authors contributed equally: Laurence de Leval, Philippe Gaulard. ✉email: philippe.gaulard@aphp.fr

Received: 4 October 2021 Accepted: 26 January 2022

Published online: 17 March 2022

constitutively express TIA-1. By contrast, perforin and granzymes expression is inducible after cell activation, and correlates with cytolytic activity⁶.

T and NK lymphocytes endowed with this cytotoxic capacity represent the normal counterpart of cytotoxic T- and T/NK-cell lymphomas. These neoplasms are commonly extranodal, following the normal distribution of cytotoxic lymphocytes within skin, spleen, upper respiratory, and gastrointestinal tracts. At these sites, the cytotoxic cells are chronically exposed to a wide diversity of antigens. This might in part explain the activated cytotoxic phenotype observed in several distinct NK/T-cell malignancies such as extranodal NK/T-cell lymphoma, nasal-type (ENKTCL), intestinal T-cell lymphomas, and primary cutaneous gamma-delta T-cell lymphoma^{1,7}.

A cytotoxic immunophenotype is also characteristic of anaplastic lymphoma kinase (ALK)-positive and most ALK-negative anaplastic large cell lymphomas (ALCL). Regarding the notably heterogeneous group of peripheral T-cell lymphomas, not otherwise specified (PTCL, NOS), few studies, mostly from Asia, described the expression of at least one cytotoxic molecule in 24–38% of cases^{6,8,9}. In gene expression profiling studies, a signature comprising high expression of transcripts associated with cytotoxic CD8⁺ T cells was substantiated in 25% of PTCL, NOS^{10–12}. Further, these cases were essentially distributed within the molecular subgroup of PTCL, NOS characterized by a Thelper1-related signature (PTCL-TBX21 group). Besides genes related to cytotoxic function, this signature included important transcription factors for cytotoxic T-cell differentiation such as *TBX21* and *EOMES*, and a set of cytokines/receptors including CXC chemokine receptor 3 (*CXCR3*) and *interferon-γ*. Interestingly, it lacked expression of *CD56*mRNA typically associated with Epstein-Barr virus (EBV)-positive ENKTCL^{11,12}.

The clinicopathological features of nodal PTCL, NOS with cytotoxic phenotype have been mostly explored in Asian patients^{8,9,13–16}. These studies underlined the aggressive clinical course and the EBV association in up to 50% of studied cases. In addition, the patients often presented with symptoms related to hemophagocytic syndrome or disseminated intravascular coagulation. However, to the best of our knowledge, the Western series of nodal cytotoxic PTCL, NOS are lacking. In addition, the molecular mechanisms involved in the biology of these lymphomas are largely unknown.

This prompted us to undertake a comprehensive clinical, pathological and molecular approach of 54 such cases.

PATIENTS AND METHODS

Patient selection

Fifty-four patients diagnosed with nodal PTCL, NOS of cytotoxic phenotype between 2000–2019 were retrieved from the files of pathology departments of Henri Mondor University Hospital and Lausanne University Hospital, and from the Tenomic consortium of the Lymphoma Study Association (LYSA). They were selected based on the following criteria: 1) initial diagnosis made on a lymph node biopsy; 2) expression of at least one cytotoxic molecule (TIA-1, granzyme B or perforin) in >50% of tumor cells and 3) tissue availability (formalin-fixed paraffin-embedded (FFPE) and/or frozen samples) for down-stream immunophenotyping and molecular testing. All cases were reviewed and classified by three hematopathologists (PG, LdL, AN), according to the criteria of the 2017 WHO classification¹. Specific entities such as ALCL ALK⁺/-, adult T-cell leukemia/lymphoma, enteropathy-associated T-cell lymphoma (EATL), monomorphic epitheliotropic intestinal T cell lymphoma (MEITL), hepatosplenic T-cell lymphoma (HSTL), and primary cutaneous T-cell lymphomas known to express cytotoxic markers were excluded. Pathological features, clinical, laboratory findings, treatment, and outcome were collected. The study was approved by the local ethical committee (Comité de Protection des Personnes Ile-de-France IX 08-009) and the tissue samples were collected and processed following standard ethical procedures (Declaration of Helsinki 1975).

Immunohistochemistry (IHC) and in situ hybridization (ISH) studies

Immunohistochemical studies were performed on FFPE sections using routine protocols on fully automated platforms (BOND-III Autostainer, Leica Microsystems, Newcastle upon Tyne, UK, or Ventana, Benchmark XT, Tucson, AZ, USA). The antibody panel included CD2, CD3, CD4, CD5, CD7, CD8, CD30, CD56, MUM1, TIA-1, perforin, granzyme B, ALK1, TCRβF1, TCRδ, CXCR3, TBX21, GATA3, and pSTAT3, as detailed in supplemental Table S1. The scoring system used to evaluate the expression of most antibodies was as follows: score 0: <1%, score 1: 1–50%, score 2: 51–75%, and score 3: >75% positive tumor cells. The cut-off of positivity was set to ≥20% for TBX21 and CXCR3 and ≥50% for GATA3, based on the IHC algorithm proposed by Amador et al. to subclassify PTCL into TBX21 and GATA3 subtypes¹⁷. According to this IHC decisional tree, a TBX21⁺ or TBX21⁻ CXCR3⁺ PTCL will be classified into PTCL-TBX21, and a TBX21⁻ CXCR3⁻ GATA3⁺ case will be subclassified into PTCL-GATA3. Only cases with positive internal control (small T lymphocytes, histiocytes) were retained. The TCRβF1-negative cases were checked in two different laboratories.

All cases were tested for the presence of EBV by in situ hybridization using oligonucleotides complementary to EBER transcripts (Leica Biosystems).

Cases with MUM1 overexpression (>50% of tumor cells positive) by immunohistochemistry were analyzed by fluorescence in situ hybridization (FISH) for detection of rearrangements of *DUSP22-IRF4* locus on 6p25.3 using Zytolight SPEC IRF4, DUSP22 Dual Color Break Apart Probe (Zytovision GmbH, Bremerhaven, Germany) and standard techniques.

DNA and RNA extraction

DNA and RNA were extracted from whole frozen or FFPE tissue sections. For DNA extraction Qiagen QIAamp DNA FFPE Tissue Kit (Qiagen Inc., Valencia, CA) or Maxwell[®] 16 FFPE Plus LEV DNA Purification Kit (Promega) was used, according to the manufacturers' recommendations. Total RNA was extracted using Maxwell RSC RNA FFPE Purification kit (Promega).

PCR for T-cell receptor gene rearrangements

Clonality was studied by multiplex PCR targeting the T-cell receptor (TR) genes (TRB and TRG), using Biomed-2 primers or using a GC-clamp multiplex polymerase chain reaction-g-denaturing gradient gel electrophoresis procedure as previously reported^{18–20}.

Targeted deep sequencing (TDS) and somatic variant filtering

A total of 33 samples with at least 20% tumor cell content and available DNA were analyzed by targeted deep sequencing (TDS) using a customized panel covering 27 genes relevant to PTCL biology (*ARID1A*, *ATM*, *BCOR*, *CARD11*, *CCR4*, *CD28*, *CTNNB1*, *DDX3X*, *DNMT3A*, *FYN*, *IDH2*, *IRF4*, *JAK1*, *JAK3*, *KMT2D*, *PIK3CD*, *PLCG1*, *PRKCB*, *RHOA*, *SETD2*, *SOC1*, *STAT3*, *STAT5B*, *TET2*, *TNFRSF1B*, *TP53*, *VAV1*). Library preparation, sequencing (MiSeq technology, Illumina, San Diego, CA) and analysis were performed as previously described¹⁹. Sequence analysis was based on established algorithms and pipelines according to GATK best practices (The Genome Analysis Toolkit) standards. The average depth of sequencing was 2348X (range 660–3345X). Briefly, forward and reverse reads were aligned to the hg19 human genome (GATK repository, build 37 decoy) using BWA aligner (v0.7.5a). BAM files were subjected to PCR duplicate removal (Picard v1.119), followed by realignment around indels and base recalibration using GATK tools (v3.7). Single nucleotide and indel variant calling were performed using samtools mpileup (v1.2) and VarScan (v2.3.7) as well as MuTect2 algorithm (GATK v3.7). The union of the variant calls were annotated for presence in dbSNP, ExAC (r.1), and COSMIC (v88) databases as well as mutation effect on gene transcript by SnpEff (v.4.3t). Further variant filtering was carried out in R, keeping variants that showed an allele frequency (VAF) > 1%, having at least 50 reads supporting the reference sequence and more than 5 reads supporting the variant. A filter based on a list of known artefacts was also applied. All retained alterations were confirmed by visual inspection with the Integrative Genomics Viewer (IGV) tool.

The impact of mutations on protein function was assessed by consulting public databases, such as ClinVar, LOVD, COSMIC, The Clinical Knowledgebase (CKB), OncoKB and literatures. Variant spliceogenicity was predicted in silico using the SPiCE algorithm (Novel diagnostic tool for prediction of variant spliceogenicity derived from a set of 395 combined in silico/in vitro

Table 1. Demographic features, presentation, and outcome of patients with nodal PTCL, NOS with cytotoxic phenotype.

Features	n	%
Gender	54	
M	39	72%
F	15	28%
Age (years)	54	
≤60	28	52%
>60	26	48%
Clinical stage	49	
I	3	6%
II	1	2%
III	7	14%
IV	38	78%
Performance status	41	
0-1	27	66%
2-4	14	34%
B symptoms	46	
yes	31	67%
no	15	33%
LDH	41	
increased	32	78%
normal	9	22%
IPI	40	
0-2	15	38%
3	12	30%
4-5	13	33%
PIT	37	
0-2	22	59%
3-4	15	41%
Hemoglobin	35	
≥10 g/dL	26	74%
<10 g/dL	9	26%
Platelets	34	
≥100 G/L	23	68%
<100 G/L	11	32%
Extranodal site(s)	46	
≥ 1 site(s)	40	87%
Medical history	51	
B-cell malignancy	10	20%
Other neoplasms	3	6%
Immune disorders	4	8%
Not significant	34	67%
Treatment	48	
CHOP-like therapy	38	79%
others	6	13%
absence of treatment	4	8%
HSCT	48	
autologous	7	
allogeneic	8*	
Outcome	50	
Alive	15	30%
Complete Remission	9	18%

Table 1. continued

Features	n	%
Died	35	70%
Lymphoma and/or infection and/or treatment-related toxicity	31	62%
2 yr OS	44%	
5 yr OS	22%	
median OS	12,7 months	

PTCL, NOS peripheral T-cell lymphoma, not otherwise specified, M male, F female, IPI International Prognostic Index, PIT Prognostic Index for T-cell lymphoma, CHOP cyclophosphamide, doxorubicin, vincristine, and prednisone, HSCT haematopoietic stem cell transplantation, OS overall survival * includes 2 patients receiving tandem autologous and allogeneic HSCT, and 1 relapsing patient after autologous HSCT

studies: an international collaborative effort; Nucleic Acids Research, Volume 46, Issue 15, 6 September 2018). The variants were grouped using the ACGS class system (<https://www.acgs.uk.com/quality/best-practice-guidelines/>), while mutations of uncertain significance were further classified as deleterious or tolerated based on the consensus of 25 in-silico predictors (VarSome Pathogenicity Scores²¹). Variants were retained for further analysis only if pathogenic (class ACGS 5 and 4) or classified as deleterious by in-silico analysis (supplemental table S2).

Detection of gene fusion transcripts using a multiplexed targeted sequencing assay

A total of 43 cases were analyzed by multiplex ligation-dependent reverse transcription-polymerase chain reaction (Id-RT-PCR) based assay, followed by high-throughput sequencing as reported by Drieux et al²² to detect 55 known PTCL-associated fusion transcripts. Briefly, total mRNAs from FFPE or frozen samples were converted into cDNA by reverse transcription, followed by specific hybridization of 126 oligonucleotidic probes on targeted sequences (supplemental table S3), and ligation of adjacent probes. The PCR amplification is permitted by barcoded primers, linked to P5 and P7 adapters for the sequencing reaction using a MiSeq technology (Illumina, San Diego, CA). An "in-house" designed software was used to analyze the FASTQ files²².

Survival analysis

The overall survival (OS) was defined from date of diagnosis until date of death or last follow-up. Survival distributions were estimated with the Kaplan-Meier method using Graphpad Prism version 9 software.

RESULTS

Clinical features and course

The study cohort included 39 males and 15 females (male:female ratio = 2.6:1), with a median age of 60 years (range, 22-82 years). Clinical data and follow-up were available for 51 patients (Table 1). Ten patients (20%) had previous or concurrent history of B-cell malignancy [classical Hodgkin lymphoma ($n = 2$, one EBV-positive), diffuse large B-cell lymphoma ($n = 5$, 4 EBV-positive), small lymphocytic lymphoma ($n = 1$), splenic marginal zone lymphoma ($n = 1$), B-lymphoblastic lymphoma ($n = 1$)]. Three patients had another neoplasm (myelodysplastic syndrome, breast and prostate cancer, one each). The time between PTCL diagnosis and previous malignancy ranged between 7 months and 13 years (median of 3 years). Four additional patients were followed for an immune disorder (Churg-Strauss syndrome, extra-membranous glomerulonephritis, linear IgA bullous dermatosis, and limbic encephalitis, one each). Aggressive clinical parameters were commonly observed and included high stage disease (III, IV) (92%), international prognostic index (IPI) > 2 (63%), B symptoms (67%), high LDH level (78%), and cytopenia (≥1 lineage) (66%). All patients presented with lymphadenopathy. The majority of patients (40/46, 87%) had involvement of at least one extranodal site, most commonly bone marrow (23/46, 50%), spleen (15/46,

33%), and liver (8/46, 17%). Less commonly, lymphoma affected bone (13%), lung (11%), skin (7%), gastrointestinal tract (7%), ENT (ear, nose, and throat, 7%), and central nervous system (2%). In addition, 7 patients had the hemophagocytic syndrome. Circulating tumor cells and malignant ascites were documented in 4 patients each. EBV viral load was evaluated for 22 patients, 11 of them showing detectable EBV copies in the peripheral blood.

Treatment information obtained for 48 patients consisted of anthracycline-containing chemotherapy (CHOP or CHOP-like regimens) ($n = 38$, 79%), whereas six patients were treated without anthracycline and four received supportive care. Twelve patients (25%) underwent a hematopoietic stem cell transplant (HSCT): five allogeneic, four autologous, and three patients received both autologous and allogeneic HSCT. Among 50 patients with follow-up data available, 35 (70%) died, mostly of disease and/or toxicity/infections related to treatment (31/35). Of the overall deaths, 63% occurred in the first 12 months. Fifteen patients (30%) were alive with a median follow-up of 75 months (range 3–153), including 8/13 patients who had received allogeneic ($n=2$), autologous ($n=2$) or both autologous and allogeneic HSCT ($n=2$). The overall survival, represented in Fig. 1 was 44% at 2 years and 22% at 5 years, with a median overall survival of 12.7 months.

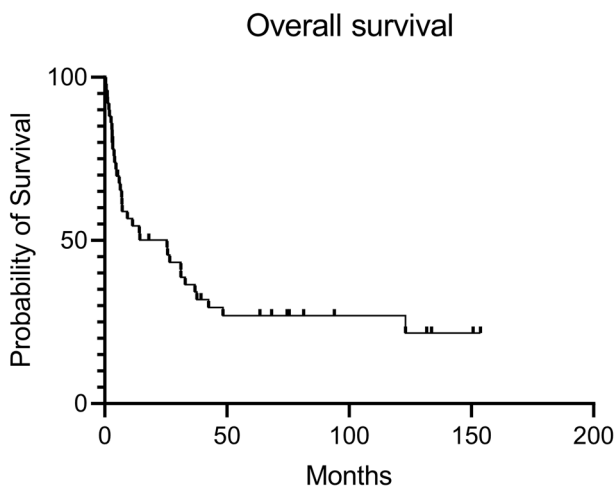


Fig. 1 Overall survival of the patients. Kaplan-Meier curve displaying overall survival of nodal peripheral T-cell lymphoma, not otherwise specified (PTCL, NOS) with cytotoxic phenotype.

Pathological features

The diagnostic tissue consisted of lymph node (LN) excisional biopsies ($n = 42$) or core biopsies ($n = 12$).

Histologically, the LNs showed total (44/54, 81%) or subtotal effacement of the architecture with remnants of residual follicles (19%). The neoplastic T cells were predominantly medium to large (70%), uncommonly small to medium (19%) or pleomorphic ranging from small to large (11%). Tumor cells with anaplastic features were observed in 4 patients (7%), scattered neoplastic T-cells with Hodgkin/Reed-Sternberg-like morphology in 8 (15%) whereas necrosis was present in 17 (31%) cases. Angiocentricity and/or angioinvasion were uncommon (5/54, 9%). Besides small non-neoplastic lymphocytes, the inflammatory background contained various amounts of histiocytes ($n = 38$, 70%), scattered eosinophils ($n = 22$, 41%) and/or plasma cells ($n = 14$, 26%). In 3 patients, numerous small clusters of epithelioid histiocytes were seen, consistent with the Lennert's variant of PTCL, NOS. For 3 other patients, the LN biopsy showed a composite T and B-cell lymphoma: 1 associating small lymphocytic lymphoma (SLL), 1 splenic marginal zone lymphoma (SMZL), and 1 EBV-negative diffuse large B cell lymphoma.

The immunophenotypic features are summarized in Fig. 2. Most cases expressed CD2 (91%) and CD3 (91%), with partial or complete loss of CD5 (64%) and/or CD7 (67%). They were commonly CD8+ (45%) or CD4-CD8- (32%) and less frequently CD4+ (15%) or CD4+CD8+ (8%). An aberrant T-cell phenotype was seen in almost all cases (50/54). Among 36 cases with both TCR β F1 and TCR δ expression status available, 17 (47%) were TCR β F1+TCR δ -, 16 (44%) TCR silent (TCR β F1-TCR δ -), 1 TCR β F1-TCR δ +, while 2 cases were TCR β F1+TCR δ +. According to the inclusion criteria, all patients expressed at least one cytotoxic molecule in > 50% of tumor cells: TIA-1 was seen in 40/46 (87%), perforin in 40/45 (89%) and granzyme B in 38/46 (83%) of analyzed cases. All, except one had an activated cytotoxic profile with the expression of perforin and/or granzyme B.

With a cut-off of positivity set to $\geq 20\%$, half of the cases (16/32) showed expression of TBX21 and 83% (34/41) were positive for CXCR3, whereas 12/34 (35%) showed GATA3 nuclear expression in $\geq 50\%$ of tumor cells. Of 38 cases evaluable along the IHC algorithm proposed by Amador *et al.* to subclassify the PTCL, NOS¹⁷, 36 cases (95%) were classified in PTCL-TBX21 subtype, and two in PTCL-GATA3 subgroup.

CD30 positivity was recorded in 36/53 cases (68%) and was usually focal and heterogeneous in intensity, with strong and uniform expression seen in three cases. Only 3/34 (9%) cases

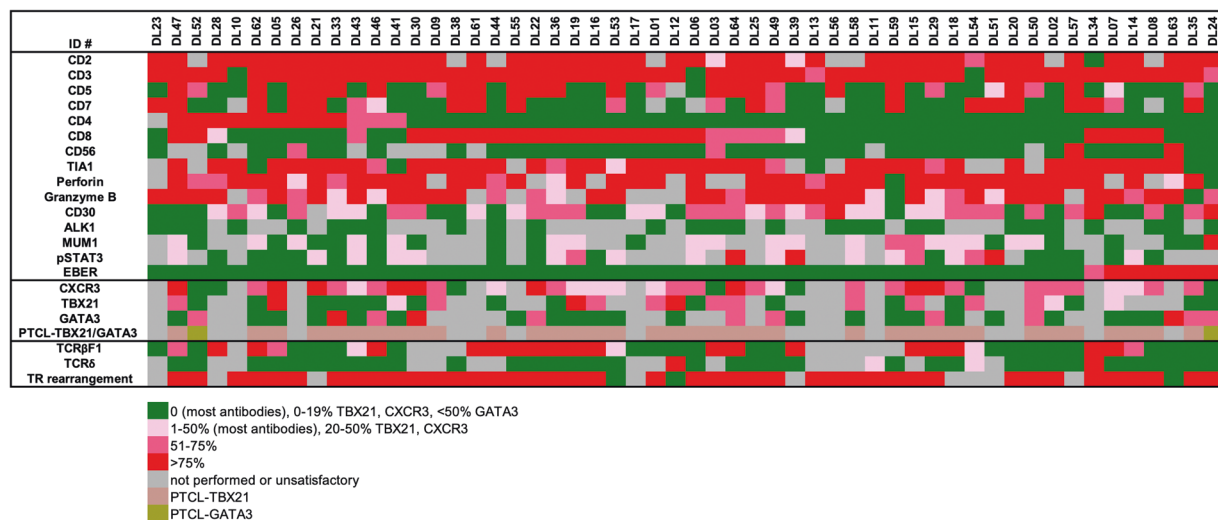


Fig. 2 Immunophenotypic features. Heatmap illustrating the immunophenotype, Epstein-Barr virus in situ hybridization (EBER) and T-cell receptor (TR) genes rearrangement results in nodal PTCL, NOS with a cytotoxic phenotype.

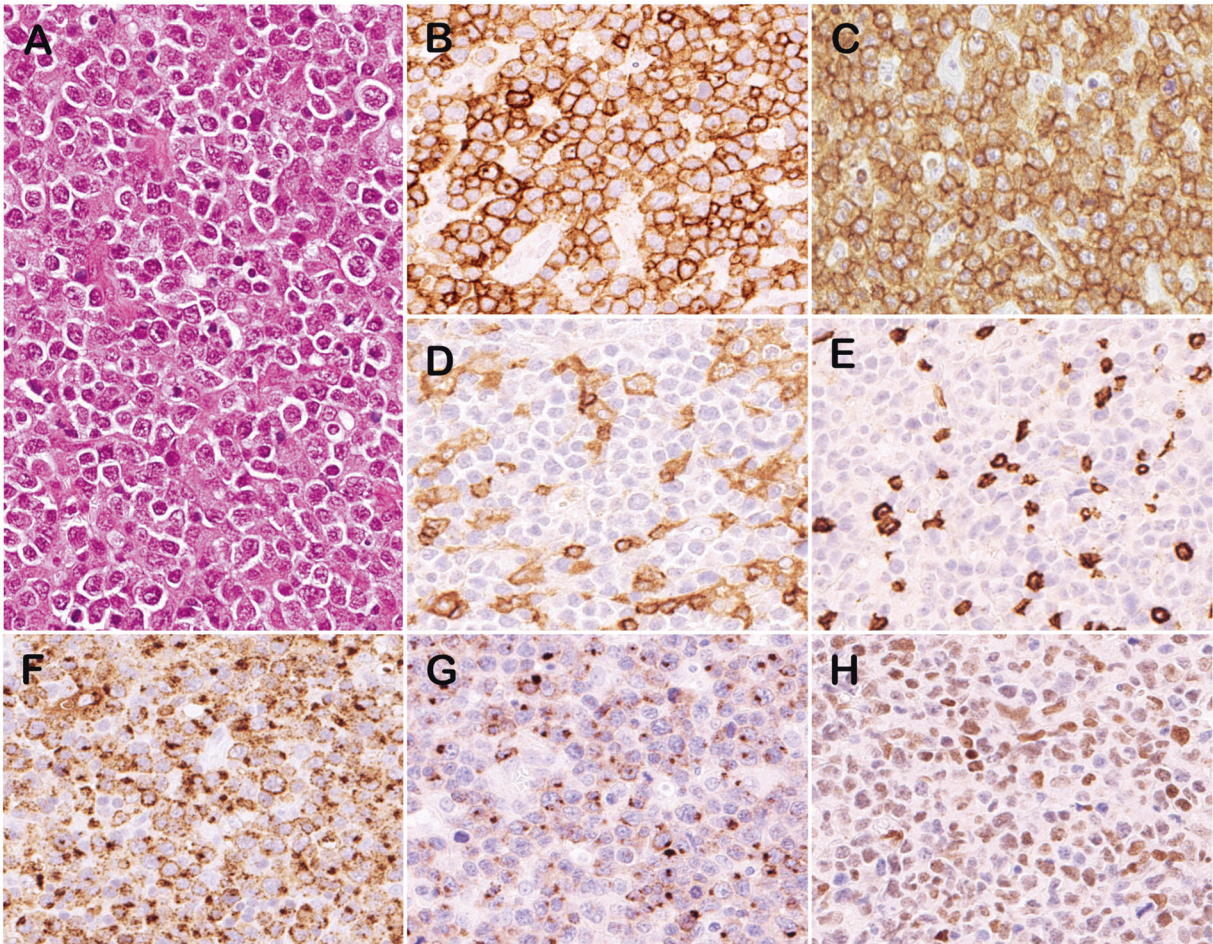


Fig. 3 Representative case of PTCL-TBX21 subtype (DL15, A–H). **A** H&E stain shows diffuse proliferation of atypical large lymphocytes with abundant cytoplasm. The neoplastic cells were positive for CD2 (**B**) and TCRβF1 (**C**) and negative for CD4 (**D**) and CD8 (**E**). They showed an activated cytotoxic phenotype with expression of granzyme B (**F**). In addition, the atypical cells were positive for CXCR3 (**G**) and heterogeneously expressed pSTAT3 (**H**) in the absence of *STAT3* gene mutations. Stains original magnification, $\times 400$, H&E hematoxylin and eosin.

contained $>50\%$ of MUM1-positive tumor cells, from which two lacked *IRF4* rearrangements and one was inadequate by FISH studies. Lastly, 4/44 (9%) were CD56 positive, 4 cases disclosed aberrant expression of CD20 and none expressed ALK1 (0/28).

EBV was absent in 39/54 patients, whereas eight patients had rare, scattered EBV-positive cells, most likely corresponding to bystander EBV infected cells. However, seven other patients showed EBV positivity in virtually all tumor cells.

Representative illustrations of morphological and phenotypical aspects of nodal, cytotoxic PTCL, NOS are shown in Figs. 3 and 4

TR clonality and genetic aberrations detected by Id-RT-PCR and TDS

Results are shown in Figs. 2 and 5. PCR analysis revealed dominant clonal TR rearrangements sometimes within a polyclonal background in 42/45 tested cases including 13/16 TCR silent cases by IHC and 6/7 EBV-positive cases.

A fusion transcript was detected in 10/43 (23%) tested cases by Id-RT-PCR assay. Six involved *VAV1* with different partners [*THAP4* ($n = 3$), *STAP2*, *HNRNPM*, *SKAP2*]. Two cases harbored *ICOS_CD28* and one case each had *ITK_SYK* and *CD58_NECTIN2* fusion transcripts.

TDS performed on 33 cases identified a total of 93 variants in 31 cases (Supplemental Table S2). These included 48% missense, 27% frameshift, 18% nonsense, 5% splice-site, and 2% in-frame insertions/deletions/duplications. Two-thirds (24/31) of mutated

cases had ≥ 2 mutations and two cases showed no mutation in analyzed genes.

Altogether, TDS and Id-RT-PCR assays identified highly recurrent mutations in epigenetic modifiers (24/33, 73%). They were followed by alterations in TCR signaling (12/33, 36%) and members of the JAK/STAT pathway (8/33, 24%). Of note, 13/33 patients (39%) had concurrent epigenetic alterations and genomic changes affecting TCR ($n = 9$) and/or JAK/STAT signaling pathways ($n = 5$). In addition, as shown in supplemental figure S1, the mean VAFs of *TET2* and *DNMT3A* was higher than that of signaling genes in those cases where two types of alterations coexisted ($p = .01$).

The most commonly mutated genes were *TET2* in 20/33 patients (61%), and *DNMT3A* in 13/33 patients (39%), two genes involved in the regulation of DNA methylation and hydroxymethylation. Ten cases harbored both *TET2* and *DNMT3A* mutations. Most *TET2* mutated cases (14/20) carried two mutations, in various combinations (Fig. 5). *KMT2D* (also known as *MLL2*), which codes for a histone-lysine N-methyltransferase, was mutated in 3/33 cases (9%); less commonly *SETD2* (6%) and *BCOR* (3%) gene mutations were encountered. Interestingly, the presence of *TET2* and/or *DNMT3A* mutations did not correlate with CD4 expression [$p = 1.0$ (Fisher exact test)] and there were no significant differences in morphology, immunophenotype and EBV status according to mutation status in epigenetic genes (supplemental Table S4)

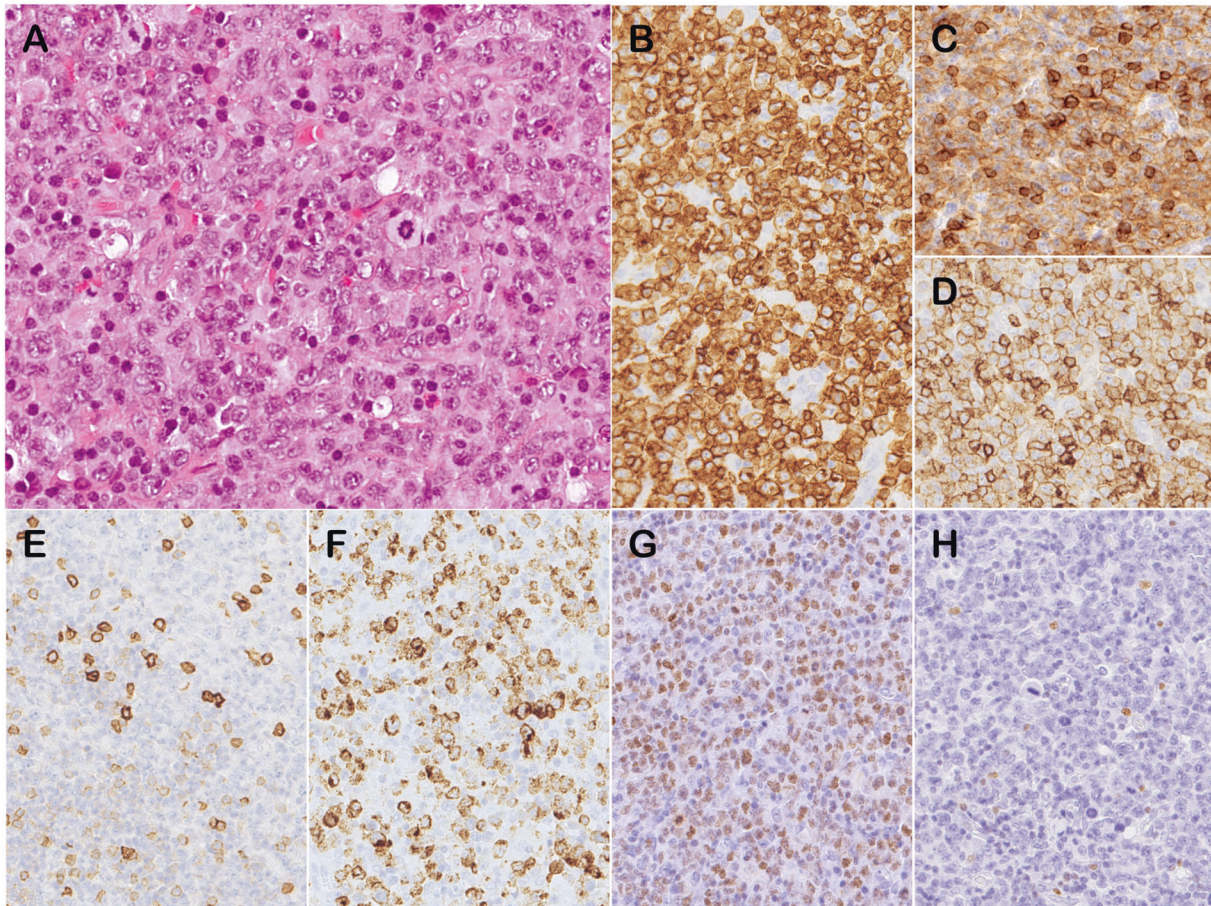


Fig. 4 Representative case of PTCL-GATA3 subtype (DL52, A–H). **A** On H&E section, the lymph node showed atypical lymphoid infiltrate composed of large cells with vesicular nuclei and conspicuous nucleoli. Scattered eosinophils are associated. The neoplastic cells were positive for CD3 (**B**), CD4 (**C**), CD8 (**D**), and showed loss of CD5 (**E**). They strongly expressed granzyme B (**F**) and showed nuclear positivity for GATA3 (**G**) with negativity for TBX21 (**H**). Stains original magnification, $\times 400$, H&E hematoxylin and eosin.

Alterations in genes related to TCR signaling were observed in 12/33 cases (36%). Most commonly involving *VAV1* in 5 cases [15%; 4 by gene fusion and 1 by inframe mutation (V778_F784del)], followed by *PLCG1* gene mutation in four cases (12%; G869E, R48W ($n = 3$)), among which one showed comutations in *PRKCB* and *CARD11* genes. In addition, two cases (6%) carried an *ICOS_CD28* fusion associated with a CD28 (D124E) gene mutation in one case. Lastly, one case each had a *FYN* or *IRF4* mutation.

Among the nine gene mutations affecting JAK/STAT pathway, observed in 8/33 patients (24%), most commonly *STAT3* ($n = 4$) or *STAT5B* ($n = 3$) genes were involved. One case each harbored a *SOCS1* or *JAK3* mutation. All *STAT3*, *STAT5B* and *JAK3* mutations were missense mutations, occurring at hotspots and functionally characterized as gain-of function^{23,24}. All these mutations were mutually exclusive except for one case in which *STAT5B* and *JAK3* mutations co-occurred. *JAK1* was wild-type in all samples. Three of the four *STAT3* mutated cases showed expression of the pSTAT3 protein by immunohistochemistry. In addition, most neoplastic lymphocytes were pSTAT3 positive in the sole *SOCS1* mutated case (DL64).

Finally, 6/33 (18%) patients had *TP53* gene mutations; all except one were missense and occurred at various genomic positions. Five of these patients with available outcome deceased, with median OS of 4 months (range 1, 7–6, 3 months).

No case showed *RHOA* or *IDH2* gene alterations characteristically found in angioimmunoblastic T-cell lymphoma (AITL) and other T_{FH} lymphomas.

Nodal cytotoxic peripheral T-cell lymphomas EBV-positive

As previously mentioned, seven patients showed EBV positivity in almost all tumor cells. Their clinico-pathological features are summarized in Table 2. There were five males and two females with a median age of 50 years (range 22–81). All presented with lymphadenopathy. Of the six patients with clinical data available, five had stage III-IV disease, four B-symptoms, four high LDH level, and three showed cytopenia of ≥ 1 lineage. At clinical staging, three patients showed ENT involvement, two of them with past history of classical Hodgkin lymphoma and DLBCL EBV+ respectively. Five out of six patients with available outcome died of disease ($n = 3$) or treatment related complication ($n = 2$), with a median survival of 31 months (range 1–123).

Histologically, these cases featured exclusively medium to large cytormorphology, with a polymorphic microenvironment in 3 cases, extensive necrosis in 3 cases, and angiocentric pattern in 2. The immunophenotype and molecular features are shown in Fig. 2 and Fig. 5, respectively and a representative case (DL08) is displayed in Fig. 6. All cases had an activated cytotoxic phenotype. Four were CD8-positive and only one stained for CD56. Four each showed CD30 expression and/or were CXCR3 positive. Four cases were TCR silent, 2 expressed TCR β F1 and 1 was TCR β F1 + δ +. Six of 7 tested cases showed a monoclonal TCR rearrangement. None of the 5 cases analyzed by Id-RT-PCR assay showed a fusion transcript. The somatic mutations observed in EBV+ cases ($n=6$) were overall similar to those EBV-, except for a single case harboring concurrent *STAT5B* and *JAK3* mutations, which was a unique configuration in the cohort.

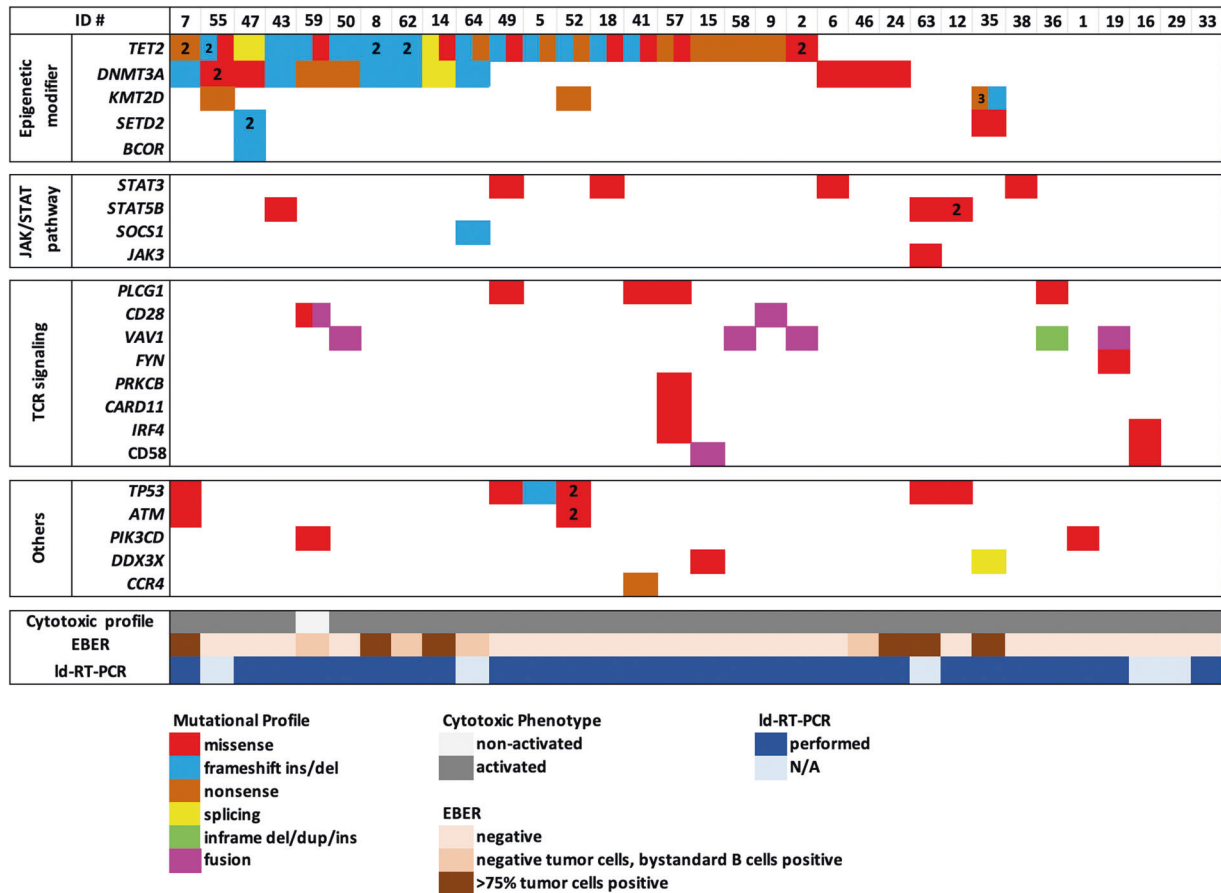


Fig. 5 Genetic features. Heatmap illustrating the Molecular alterations in 33 patients with nodal PTCL, NOS with cytotoxic phenotype by targeted deep sequencing (TDS) and ligation-dependent reverse transcription-polymerase chain reaction (Id-RT-PCR) assay.

DISCUSSION

We report here the clinicopathologic features of a Western series of 54 patients with nodal PTCL, NOS of cytotoxic phenotype, associated with settings suggestive of immune dysregulation in a proportion of them. In addition, we describe for the first time their molecular profile which revealed frequent alterations in epigenetic modifiers, TCR signaling and JAK/STAT pathway.

Except for the cytotoxic phenotype, cytotoxic PTCL, NOS evaluated here remain morphologically heterogeneous, showing overlapping features with PTCL, NOS in general^{1,3}. They often displayed a diffuse effacement of nodal architecture by medium/large atypical lymphocytes in a variable microenvironment and uncommonly had features consistent with the Lennert's variant of PTCL, NOS. These findings are in keeping with those previously reported in Asian patients^{8,9,16}.

Most cases appear derived from mature T lymphocytes, more commonly $\alpha\beta$ -T cells and rarely $\gamma\delta$. Evidence of T-cell origin was documented in all except one TCR silent cases tested, which disclosed clonal TR rearrangements. Therefore, a NK cell origin can be ruled out in almost all cases and cannot explain the high rate of TCR silent cases observed in our study (44%) compared with the lower rate reported in PTCL comprising all subtypes (20%) and even in nodal EBV-negative cytotoxic PTCL (25%)^{7,16}. In addition, nearly half of our series were CD8+ (45%) and some either CD4+ (15%) or CD4+CD8+ (8%). This heterogeneous phenotype of nodal cytotoxic PTCL, NOS might reflect the diversity of mature normal cytotoxic lymphocytes. Cytotoxic lymphocytes in lymph nodes are largely represented by CD8+ cytotoxic T-lymphocytes (CTL) and infrequently by cytotoxic effectors of innate immune system such as NK and $\gamma\delta$ -T cells. However, CD4+T cells

endorsed with cytotoxic activity can be generated under various inflammatory conditions or by virus infection and appear to manifest complementary functions to CD8+CTLs in vivo²⁵. Furthermore, a subset of $\alpha\beta$ CD4-CD8- double-negative T cells has been described to be involved in anti-tumor immunity, acting as regulatory T cells and/or cytotoxic T cells^{26,27}.

Furthermore, our data support that most of these lymphomas are developed from activated/effector cytotoxic T cells showing a Th1-like phenotype and lacking the NK-associated marker CD56. Indeed, all except one case showed an activated cytotoxic phenotype with expression of perforin and/or granzyme B. In addition, 95% of our cases were subclassified into PTCL-TBX21 group following the immunohistochemical algorithm proposed by Iqbal's group based on CXCR3, TBX21 and GATA3 protein expression¹⁷. CXCR3 is regarded as a selective marker of Th1 lymphocytes and although non-specific for cytotoxic T cells²⁸, its high expression by immunohistochemistry has been already reported in nodal cytotoxic PTCL⁸. In addition, the gene signature of cytotoxic T-cell lymphoma subset detached from the PTCL-TBX21 group of PTCL, NOS showed besides TBX21, high levels of CXCR3¹⁰⁻¹².

Although the genomic landscape of nodal PTCL, NOS has been previously explored^{10,29-31}, our study is the first to describe the molecular abnormalities in those with cytotoxic phenotype. Overall, the genetic landscape showed frequent mutations in epigenetic modifiers, and their common association with abnormalities in TCR and JAK/STAT signaling, irrespective of the EBV status. Three quarters of cases (73%) revealed mutations in *TET2* (61%) or *DNMT3A* (39%) regulating DNA methylation and hydroxymethylation. Of note, mutations in these two genes

Table 2. Clinico-pathological features of EBV + nodal PTCL, NOS with cytotoxic phenotype.

ID #	DL07	DL08	DL14	DL24	DL34	DL35	DL63
Sexe	F	M	F	M	M	M	M
Age	57	81	66	50	22	48	34
Stage	III	IV	IV	I	III	IV	na
Extranodal sites	ENT	ENT	ENT, BM	–		Liver, BM	na
B-symptoms	+	+	+	–	+	–	na
LDH (increased)	+	+	+	na	+	–	na
IPI	2	4	3	na	2	2	na
Cytopenia ≥ 1 lineage	–	+	+	na	+	–	na
Medical history	CHL	–	DLBCL EBV +, AHAI	B hepatitis	glomerulonephritis	–	na
Reccurrence of disease in the LN	na	na	LN cervical	na	LN mediastinal	LN (NOS)	na
Treatment	chemo	no treatment	chemo	chemo	chemo + allo HSCT	chemo +allo HSCT	na
OS time (months)	3	37	25	1	123	75	na
Outcome	DOD	DOD	Died of treatment retated complication (infection)	Died of treatment retated complication (infection)	DOD	alive	na
LN site biopsy	not specified	peripancreatic	axillary	cervical	cervical	mesenteric	cervical
Infiltration pattern	diffuse	diffuse	diffuse	diffuse	diffuse	interfollicular	diffuse
Tumor cell size	medium to large	medium to large	medium	large	medium to large	medium to large	large
Necrosis	++	++	–	+	++	–	–
Angiocentricity	+	–	–	–	+	–	–
Microenvironment	histiocytes	0	polymorphic	0	polymorphic	polymorphic	histiocytes

PTCL, NOS peripheral T-cell lymphoma, not other specified, EBV Epstein Barr virus, LDH lactate dehydrogenase, IPI International Prognostic Index, ENT ear, nose, throat, BM bone marrow, CHL classical Hodgkin lymphoma, DLBCL diffuse large B-cell lymphoma, AHAI autoimmune hemolytic anemia, LN lymph node, allo HSCT allogeneic hematopoietic stem cell transplantation, chemo chemotherapy, OS overall survival, DOD died of disease

frequently co-occurred, suggesting an oncogenic cooperation of these genes, as observed in AITL and other T_{FH} lymphomas^{32,33}. Interestingly, the mean VAF of *TET2* and *DNMT3A* mutations were elevated (35 and 28%, respectively) and the VAF of these two genes were significantly higher than the VAF of genes involved in TCR and JAK/STAT signaling in cases bearing both epigenetic and signaling alterations ($p = .01$) (Supplemental Fig. 1). This suggests that epigenetic changes could be the first step in the oncogenic process of this neoplasm, with their possible occurrence in a hematopoietic progenitor, as described in PTCL of T_{FH} origin^{32–35} and recently in another cytotoxic entity, i.e., chronic NK lymphoproliferative disorders³⁶. Our observations extend the notion that epigenetic disturbances in hematopoietic stem cells might represent a common ground to the development of various types of T-cell lymphomas and might explain the diversity of T-cell lymphoma phenotype in regard to CD8/CD4 expression seen in our series (supplemental table S4)^{31,32,35,37–40}. Although nonspecific, these recurrent epigenetic alterations seen in our patients may bring the rational of testing epigenetic targeting drugs, such as 5 azacytidine or romidepsin, as proposed for AITL and PTCL, NOS^{41–44}.

Apart from epigenetic changes, we identified alterations in costimulatory/TCR-related signaling genes in 36% of nodal PTCL, NOS with cytotoxic phenotype. Mutations or chromosomal translocations implicating *VAV1*, *PLCG1*, and *CD28* genes were the most frequent events. *VAV1_THAP4* gene fusion observed in three patients, were first reported by Abate *et al.* in PTCL, NOS

who showed an increased activation of VAV1 effector pathways MAPK and JNK⁴⁵. Furthermore, two cases showed *CD28_ICOS* gene fusion, one of them carrying in addition, CD28 D124E missense mutation. These gain-of-function mutation and fusion transcript which lead to enhancement of CD28 intracellular signaling and up-regulation of downstream genes involved in PI3K, MAPK or NF-κB signaling, have been mostly described in T_{FH}-derived lymphomas^{46–48}. Moreover, one of the four *PLCG1* mutated cases carried the variant G869E described as functionally activating in AITL⁴⁸. Collectively, our data expand the spectrum of PTCLs characterized by deregulated TCR signaling activation, which likely represents an oncogenic mechanism and might predict early treatment failure with anthracyclin-based chemotherapy⁴⁸.

Although the genomic alterations found in nodal PTCL, NOS with cytotoxic phenotype are largely overlapping with those described in other PTCL subtypes, the frequency of their occurrence differs. The high recurrence of *TET2* and *DNMT3A* mutations observed by us contrasts to the low rate (<15%) of these mutations detected in ENKTCL, MEITL, ALCL, ALK-negative, HSTL^{38,39,49,50}. By contrary, *SETD2* genomic changes and subversion of cytokine receptor signaling by mutation in members of JAK/STAT pathway appears less prominent in nodal than in extranodal cytotoxic T-cell lymphomas. One-fourth of our patients had mutations in members of JAK/STAT pathway. This frequency is more in keeping with nodal ALCL, ALK-negative (15–30%)^{51,52} but inferior to that reported in HSTL (45%)^{38,53}, intestinal T-cell

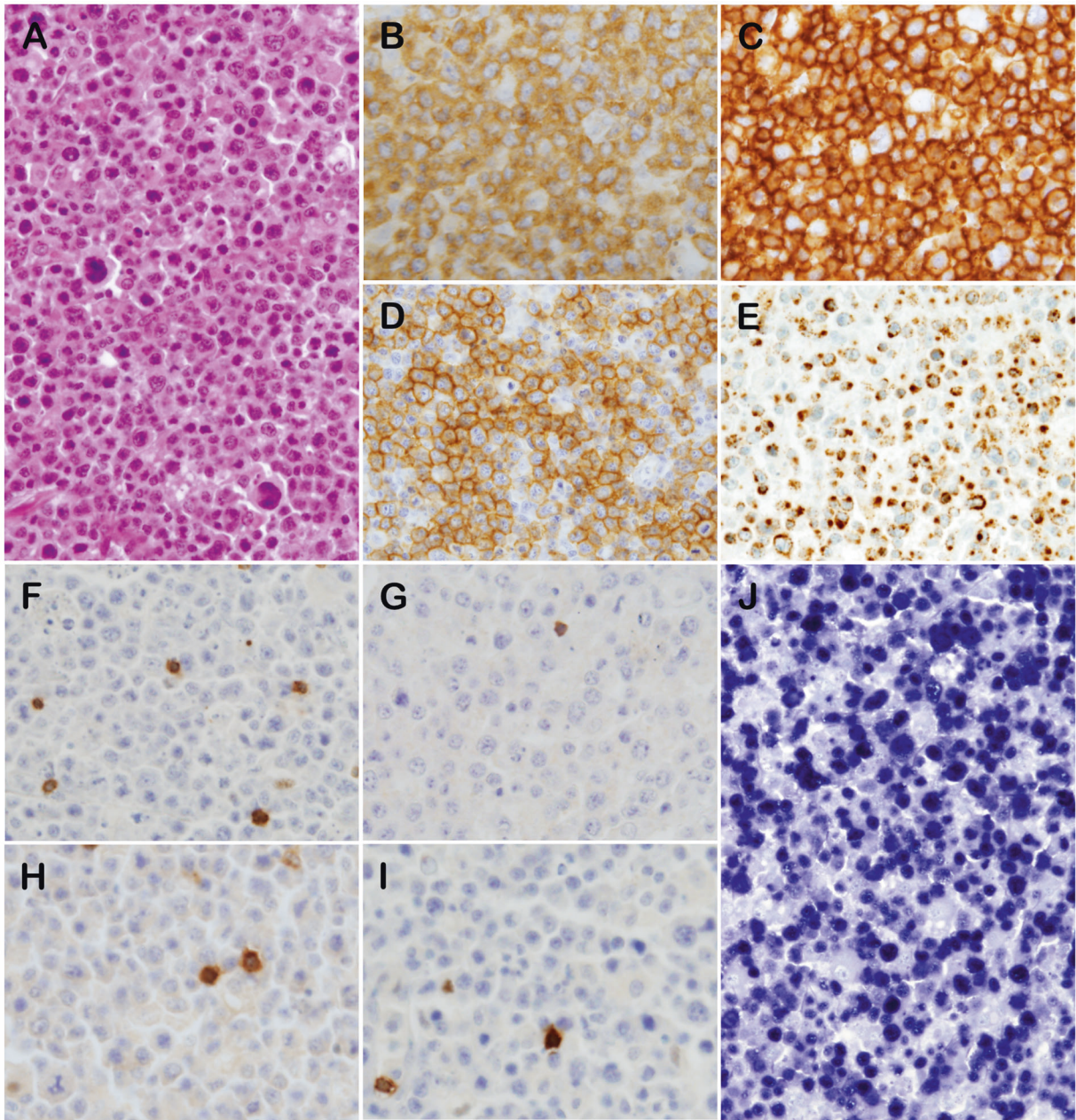


Fig. 6 Representative cases of Epstein-Barr virus (EBV)-positive nodal cytotoxic peripheral T-cell lymphoma, not otherwise specified (PTCL, NOS) (DL08, A–J). **A** The lymph node showed diffuse proliferation of pleomorphic, mitotically active lymphoid cells on H&E stain. They expressed cytoplasmic CD3 (**B**), CD8 (**C**), CD30 (**D**), and granzyme B (**E**). The atypical lymphocytes were negative for CD5 (**F**), CD56 (**G**), TCRβF1 (**H**), TCRδ (**I**). Virtually all neoplastic lymphocytes were EBER positive (**J**). Stains original magnification, $\times 400$, H&E hematoxylin and eosin.

lymphomas (65–80%)^{39,54,55}, large granular lymphocytic leukemia (70%)⁵⁶ and breast implant-associated ALCL (59%)⁵⁷. The same holds true for *SETD2*, found mutated in only two of our patients as opposed to 30 or 93% rate observed in HSTL and MEITL respectively^{38,55}. These data might reflect the differences in the presumptive cell of origin of these lymphomas, in their micro-environmental niche and in the pathogenic cues.

Interestingly, one third of our patients had previous or concomitant B-cell malignancies from which 5 EBV-related, (20%) immune disorders (8%) or other malignancies (6%), suggesting that immune dysfunction might contribute to nodal cytotoxic PTCL, NOS lymphomagenesis. In the study of Nijland et al. 12% of PTCL, some with cytotoxic phenotype, occurred in immunocompromised patients⁵⁸. Furthermore, in their meta-

analysis of 605 immunodeficiency-related PTCL cases, autoimmune diseases (24%) and hematologic malignancies (9%) were between the most common underlying disorders. It has been shown that underlying immunodeficiency constitutes a risk factor for PTCL development and chronic viral, tumoral, or exogenous antigen exposure, prolonged treatment with immunosuppressive or chemotherapeutic drugs associated with decreased immunosurveillance contribute to this risk^{1,7,58–61}. Chronic contact of CTLs to exogenous proteins such as gliadin or to EBV antigens at the mucosal sites is a well-documented pathogenic trigger in EATL and ENKTCL^{1,7}.

Finally, EBV infection may be involved in the biology of a small subset of nodal cytotoxic T-cell lymphomas, with 7 patients (13%) disclosing EBV in virtually all tumor cells. This rate of EBV infection

is similar to that reported in PTCL, NOS coming from Western countries^{3,62} but lower than in Asian series (28–51%)^{9,13–16}, likely reflecting EBV infection's epidemiology. Though the diagnosis was made on a lymph node biopsy in all of our patients, three showed ENT disease manifestation at imaging staging, raising the possibility of nodal involvement by an ENKTCL. However, most cases showed atypical features for ENKTCL. They had commonly a CD8+, CD56- phenotype, and clonal TR rearrangement, with 2 patients showing unusual association with classical HL or EBV+ DLBCL. Therefore, these findings reinforce the previous reports that EBV+ nodal, cytotoxic T/NK lymphomas are distinct from ENKTCL^{1,13–16,63}. Nevertheless, to achieve this diagnosis testing every case of PTCL for EBV with sensitive EBER ISH method is required as well as a complete work-up of patients to ensure for the absence of extranodal disease, at diagnosis.

Overall, we show here that patients with nodal PTCL, NOS with a cytotoxic phenotype have an unfavorable outcome in keeping with previous reports^{7–9,11–13,15,16}, however, without significant differences as compared with PTCL, NOS^{64,65}. These lymphomas frequently present within a background of impaired immunity, although rarely associate an EBV infection. They show an activated cytotoxic phenotype and fit into the PTCL-TBX21 subgroup. The mutational profile highlights recurrent epigenetic alterations and abnormalities in TCR-related signaling genes, with JAK/STAT pathway mutations seen less commonly than in extra-nodal cytotoxic PTCL. This suggests that alterations in epigenetics and cell-signaling pathways may play a critical role in their pathobiology and offers the rationale for investigating epigenetic modulators or cell signaling inhibitors in these patients with a dismal prognosis.

REFERENCES

- WHO classif 2016 TJ. *WHO Classification of Tumours of Haematopoietic and Lymphoid Tissues*. Revised 4th Edition, Volume 2.
- Laurent, C. et al. Impact of Expert Pathologic Review of Lymphoma Diagnosis: Study of Patients From the French Lymphopath Network. *J. Clin. Oncol.* **35**, 2008–2017 (2017).
- Weisenburger, D. D. et al. Peripheral T-cell lymphoma, not otherwise specified: a report of 340 cases from the International Peripheral T-cell Lymphoma Project. *Blood* **117**, 3402–3408 (2011).
- Trapani, J. A. & Smyth, M. J. Functional significance of the perforin/granzyme cell death pathway. *Nat. Rev. Immunol.* **2**, 735–747 (2002).
- Sánchez-Jiménez, C. & Izquierdo, J. M. T-cell intracellular antigens in health and disease. *Cell Cycle* **14**, 2033–2043 (2015).
- Kanavaros, P., Boulland, M. L., Petit, B., Arnulf, B. & Gaulard, P. Expression of cytotoxic proteins in peripheral T-cell and natural killer-cell (NK) lymphomas: association with extranodal site, NK or Tgammadelta phenotype, anaplastic morphology and CD30 expression. *Leuk. Lymphoma*. **38**, 317–326 (2000).
- Swerdlow, S. H. et al. Cytotoxic T-cell and NK-cell lymphomas: current questions and controversies. *Am. J. Surg. Pathol.* **38**, e60–e71 (2014).
- Asano, N. et al. Linkage of expression of chemokine receptors (CXCR3 and CCR4) and cytotoxic molecules in peripheral T cell lymphoma, not otherwise specified and ALK-negative anaplastic large cell lymphoma. *Int. J. Hematol.* **91**, 426–435 (2010).
- Asano, N. et al. Clinicopathologic and prognostic significance of cytotoxic molecule expression in nodal peripheral T-cell lymphoma, unspecified. *Am. J. Surg. Pathol.* **29**, 1284–1293 (2005).
- Heavican, T. B. et al. Genetic drivers of oncogenic pathways in molecular subgroups of peripheral T-cell lymphoma. *Blood* **133**, 1664–1676 (2019).
- Iqbal, J. et al. Gene expression signatures delineate biological and prognostic subgroups in peripheral T-cell lymphoma. *Blood* **123**, 2915–2923 (2014).
- Iqbal, J. et al. Molecular signatures to improve diagnosis in peripheral T-cell lymphoma and prognostication in angioimmunoblastic T-cell lymphoma. *Blood* **115**, 1026–1036 (2010).
- Kato, S. et al. T-cell receptor (TCR) phenotype of nodal Epstein-Barr virus (EBV)-positive cytotoxic T-cell lymphoma (CTL): a clinicopathologic study of 39 cases. *Am. J. Surg. Pathol.* **39**, 462–471 (2015).
- Kato, S. et al. Nodal cytotoxic molecule (CM)-positive Epstein-Barr virus (EBV)-associated peripheral T cell lymphoma (PTCL): a clinicopathological study of 26 cases. *Histopathology* **61**, 186–199 (2012).
- Ng, S.-B. et al. Epstein-Barr virus-associated primary nodal T/NK-cell lymphoma shows a distinct molecular signature and copy number changes. *Haematologica* **103**, 278–287 (2018).
- Yamashita, D. et al. Reappraisal of nodal Epstein-Barr Virus-negative cytotoxic T-cell lymphoma: Identification of indolent CD5+ diseases. *Cancer Sci.* **109**, 2599–2610 (2018).
- Amador, C. et al. Reproducing the molecular subclassification of peripheral T-cell lymphoma-NOS by immunohistochemistry. *Blood* **134**, 2159–2170 (2019).
- Theodorou, I. et al. VJ rearrangements of the TCR gamma locus in peripheral T-cell lymphomas: analysis by polymerase chain reaction and denaturing gradient gel electrophoresis. *J. Pathol.* **178**, 303–310 (1996).
- Trimech, M. et al. Angioimmunoblastic T-Cell Lymphoma and Chronic Lymphocytic Leukemia/Small Lymphocytic Lymphoma: A Novel Form of Composite Lymphoma Potentially Mimicking Richter Syndrome. *Am. J. Surg. Pathol.* **45**, 773–786 (2021).
- van Dongen, J. J. M. et al. Design and standardization of PCR primers and protocols for detection of clonal immunoglobulin and T-cell receptor gene recombinations in suspect lymphoproliferations: report of the BIOMED-2 Concerted Action BMH4-CT98-3936. *Leukemia* **17**, 2257–2317 (2003).
- Kopanos, C. et al. VarSome: the human genomic variant search engine. *Bioinformatics* **35**, 1978–1980 (2019).
- Drieux, F. et al. Detection of Gene Fusion Transcripts in Peripheral T-Cell Lymphoma Using a Multiplexed Targeted Sequencing Assay. *J. Mol. Diagn.* **51525-1578**, 00124–0 (2021).
- Pizzi, M., Margolske, E. & Inghirami, G. Pathogenesis of Peripheral T Cell Lymphoma. *Annu. Rev. Pathol. Mech. Dis.* **13**, 293–320 (2018).
- Waldmann, T. A. & Chen, J. Disorders of the JAK/STAT Pathway in T Cell Lymphoma Pathogenesis: Implications for Immunotherapy. *Annu. Rev. Immunol.* **35**, 533–550 (2017).
- Takeuchi, A. & Saito, T. CD4⁺ T. L., a Cytotoxic Subset of CD4⁺ T Cells, Their Differentiation and Function. *Front. Immunol.* **8**, 194 (2017).
- Giacoma De Tullio, Pasquale Iacopino, & Attilio Guarini. The αβ-double negative T cells in lymphoma patients: the predictive role and the functional attitude. *J. Immunol.* **192**, 142.9 (2014).
- Voelkl, S. et al. Characterization of MHC class-I restricted TCRαβ+ CD4-CD8- double negative T cells recognizing the gp100 antigen from a melanoma patient after gp100 vaccination. *Cancer Immunol. Immunother.* **58**, 709–718 (2009).
- Ishida, T. et al. CXC Chemokine Receptor 3 and CC Chemokine Receptor 4 Expression in T-Cell and NK-Cell Lymphomas with Special Reference to Clinicopathological Significance for Peripheral T-Cell Lymphoma, Unspecified. *Clin. Cancer Res.* **10**, 5494–5500 (2004).
- Laginestra, M. A. et al. Correction: Whole exome sequencing reveals mutations in FAT1 tumor suppressor gene clinically impacting on peripheral T-cell lymphoma not otherwise specified. *Mod. Pathol.* **33**, 319–319 (2020).
- Ji, M.-M. et al. Histone modifier gene mutations in peripheral T-cell lymphoma not otherwise specified. *Haematologica* **103**, 679–687 (2018).
- Watatani, Y. et al. Molecular heterogeneity in peripheral T-cell lymphoma, not otherwise specified revealed by comprehensive genetic profiling. *Leukemia* **33**, 2867–2883 (2019).
- Couronné, L., Bastard, C. & Bernard, O. A. TET2 and DNMT3A mutations in human T-cell lymphoma. *N. Engl. J. Med.* **366**, 95–96 (2012).
- Lemonnier, F. et al. Integrative analysis of a phase 2 trial combining lenalidomide with CHOP in angioimmunoblastic T-cell lymphoma. *Blood Adv.* **5**, 539–548 (2021).
- Lemonnier, F., Gaulard, P. & de Leval, L. New insights in the pathogenesis of T-cell lymphomas. *Curr. Opin. Oncol.* **30**, 277–284 (2018).
- Sakata-Yanagimoto, M. et al. Somatic RHOA mutation in angioimmunoblastic T cell lymphoma. *Nat. Genet.* **46**, 171–175 (2014).
- Pastoret, C. et al. Linking the KIR phenotype with STAT3 and TET2 mutations to identify chronic lymphoproliferative disorders of NK cells. *Blood* **137**, 3237–3250 (2021).
- Lemonnier, F. et al. Recurrent TET2 mutations in peripheral T-cell lymphomas correlate with TFH-like features and adverse clinical parameters. *Blood* **120**, 1466–1469 (2012).
- McKinney, M. et al. The Genetic Basis of Hepatosplenic T-cell Lymphoma. *Cancer Discov.* **7**, 369–379 (2017).
- Moffitt, A. B. et al. Enteropathy-associated T cell lymphoma subtypes are characterized by loss of function of SETD2. *J. Exp. Med.* **214**, 1371–1386 (2017).
- Palomero, T. et al. Recurrent mutations in epigenetic regulators, RHOA and FYN kinase in peripheral T cell lymphomas. *Nat. Genet.* **46**, 166–170 (2014).
- Pro, B. et al. Romidepsin induces durable responses in patients with relapsed or refractory angioimmunoblastic T-cell lymphoma. *Hematological. Oncol.* **35**, 914–917 (2017).
- Falchi, L. et al. Combined oral 5-azacytidine and romidepsin are highly effective in patients with PTCL: a multicenter phase 2 study. *Blood* **137**, 2161–2170 (2021).

43. Coiffier, B. et al. Results from a pivotal, open-label, phase II study of romidepsin in relapsed or refractory peripheral T-cell lymphoma after prior systemic therapy. *J. Clin. Oncol.* **30**, 631–636 (2012).
44. Lemonnier, F. et al. Treatment with 5-azacytidine induces a sustained response in patients with angioimmunoblastic T-cell lymphoma. *Blood* **132**, 2305–2309 (2018).
45. Abate, F. et al. Activating mutations and translocations in the guanine exchange factor VAV1 in peripheral T-cell lymphomas. *Proc. Natl. Acad. Sci. USA* **114**, 764–769 (2017).
46. Rohr, J. et al. Recurrent activating mutations of CD28 in peripheral T-cell lymphomas. *Leukemia* **30**, 1062–1070 (2016).
47. Vallois, D. et al. RNA fusions involving CD28 are rare in peripheral T-cell lymphomas and concentrate mainly in those derived from follicular helper T cells. *Haematologica* **103**, e360–e363 (2018).
48. Vallois, D. et al. Activating mutations in genes related to TCR signaling in angioimmunoblastic and other follicular helper T-cell-derived lymphomas. *Blood* **128**, 1490–1502 (2016).
49. Crescenzo, R. et al. Convergent mutations and kinase fusions lead to oncogenic STAT3 activation in anaplastic large cell lymphoma. *Cancer Cell* **27**, 516–532 (2015).
50. Gao, L.-M. et al. Somatic mutations in KMT2D and TET2 associated with worse prognosis in Epstein-Barr virus-associated T or natural killer-cell lymphoproliferative disorders. *Cancer Biol. Ther.* **20**, 1319–1327 (2019).
51. Crescenzo, R. et al. Convergent mutations and kinase fusions lead to oncogenic STAT3 activation in anaplastic large cell lymphoma. *Cancer Cell* **27**, 516–532 (2015).
52. Lobello, C. et al. STAT3 and TP53 mutations associate with poor prognosis in anaplastic large cell lymphoma. *Leukemia* **35**, 1500–1505 (2021).
53. Nicolae, A. et al. Frequent STAT5B mutations in $\gamma\delta$ hepatosplenic T-cell lymphomas. *Leukemia* **28**, 2244–2248 (2014).
54. Nicolae, A. et al. Mutations in the JAK/STAT and RAS signaling pathways are common in intestinal T-cell lymphomas. *Leukemia* **30**, 2245–2247 (2016).
55. Roberti, A. et al. Type II enteropathy-associated T-cell lymphoma features a unique genomic profile with highly recurrent SETD2 alterations. *Nat. Commun.* **7**, 12602 (2016).
56. Küçük, C. et al. Activating mutations of STAT5B and STAT3 in lymphomas derived from $\gamma\delta$ -T or NK cells. *Nat. Commun.* **6**, 6025 (2015).
57. Laurent, C. et al. Gene alterations in epigenetic modifiers and JAK-STAT signaling are frequent in breast implant-associated ALCL. *Blood* **135**, 360–370 (2020).
58. Nijland, M. L. et al. Clinicopathological characteristics of T-cell non-Hodgkin lymphoma arising in patients with immunodeficiencies: a single-center case series of 25 patients and a review of the literature. *Haematologica* **103**, 486–496 (2018).
59. Campidelli, C. et al. Simultaneous occurrence of peripheral T-cell lymphoma unspecified and B-cell small lymphocytic lymphoma. Report of 2 cases. *Hum. Pathol.* **38**, 787–792 (2007).
60. Martinez, A. et al. Clonal T-cell populations and increased risk for cytotoxic T-cell lymphomas in B-CLL patients: clinicopathologic observations and molecular analysis. *Am. J. Surg. Pathol.* **28**, 849–858 (2004).
61. Gilardin, L. et al. Peripheral T-cell lymphoma in HIV-infected patients: a study of 17 cases in the combination antiretroviral therapy era. *Br. J. Haematol.* **161**, 843–851 (2013).
62. Went, P. et al. Marker expression in peripheral T-cell lymphoma: a proposed clinical-pathologic prognostic score. *J. Clin. Oncol.* **24**, 2472–2479 (2006).
63. Kato, S., Yamashita, D. & Nakamura, S. Nodal EBV+ cytotoxic T-cell lymphoma: A literature review based on the 2017 WHO classification. *J. Clin. Exp. Hematop.* **60**, 30–36 (2020).
64. Dobay, M. P. et al. Integrative clinicopathological and molecular analyses of angioimmunoblastic T-cell lymphoma and other nodal lymphomas of follicular helper T-cell origin. *Haematologica* **102**, e148–e151 (2017).
65. Federico, M. et al. Peripheral T cell lymphoma, not otherwise specified (PTCL-NOS). A new prognostic model developed by the International T cell Project Network. *Br. J. Haematol.* **181**, 760–769 (2018).

ACKNOWLEDGEMENTS

We thank the LYSA-Pathology and the Platform of Biological Resources from Henri Mondor University Hospital. We also thank the participants of TENOMIC consortium (a complete membership list appears in the supplemental Appendix).

AUTHOR CONTRIBUTIONS

A.N., L.dL, and P.G. performed study design, analyzed data and wrote the paper. A.N., V.F., D.L. collected data. A.N. made the figures. J.B., E.M., A.L. provided acquisition, analysis and interpretation of TDS data. E.M. provided expert statistical analysis. F.D. performed Id-RT-PCR analysis and interpreted the data. D. L. and F.L. provided clinical expertise. M.P. E.P., B.B., C.B. V.S., A. T.-G., provided patient samples and clinical information. V.F., M.-H.D.-L., and C.R. provided technical support and performed experiments. All authors read and approved the final paper.

FUNDING

This work was supported by the Institut National de la Santé et de la Recherche Médicale (INSERM), grants from Leukemia Lymphoma Society (SCOR grant - LLS SCOR 7013-17) and Institut Carnot CALYM.

ETHICS APPROVAL / CONSENT TO PARTICIPATE

The study was approved by the local ethical committee (Comité de Protection des Personnes Ile-de-France IX 08-009) and the tissue samples were collected and processed following standard ethical procedures (Declaration of Helsinki 1975).

COMPETING INTERESTS

The authors declare no competing interests.

ADDITIONAL INFORMATION

Supplementary information The online version contains supplementary material available at <https://doi.org/10.1038/s41379-022-01022-w>.

Correspondence and requests for materials should be addressed to Philippe Gaulard.

Reprints and permission information is available at <http://www.nature.com/reprints>

Publisher's note Springer Nature remains neutral with regard to jurisdictional claims in published maps and institutional affiliations.